

# Effect of Buoyancy Ratio on Non-Darcy Mixed Convection in a Vertical Channel: A Thermal Non-equilibrium Approach

Manish K. Khandelwal\*, P. Bera, and A. Chakrabarti,

**Abstract**—This article presents a numerical study of the double-diffusive mixed convection in a vertical channel filled with porous medium by using non-equilibrium model. The flow is assumed fully developed, uni-directional and steady state. The controlling parameters are thermal Rayleigh number ( $Ra_T$ ), Darcy number ( $Da$ ), Forchheimer number ( $F$ ), buoyancy ratio ( $N$ ), inter phase heat transfer coefficient ( $H$ ), and porosity scaled thermal conductivity ratio ( $\gamma$ ). The Brinkman-extended non-Darcy model is considered. The governing equations are solved by spectral collocation method. The main emphasize is given on flow profiles as well as heat and solute transfer rates, when two diffusive components in terms of buoyancy ratio are in favor (against) of each other and solid matrix and fluid are thermally non-equilibrium. The results show that, for aiding flow ( $Ra_T = 1000$ ), the heat transfer rate of fluid ( $Nu_f$ ) increases upto a certain value of  $H$ , beyond that decreases smoothly and converges to a constant, whereas in case of opposing flow ( $Ra_T = -1000$ ), the result is same for  $N = 0$  and  $1$ . The variation of  $Nu_f$  in ( $N, Nu_f$ )-plane shows sinusoidal pattern for  $Ra_T = -1000$ . For both cases (aiding and opposing) the flow destabilize on increasing  $N$  by inviting point of inflection or flow separation on the velocity profile. Overall, the buoyancy force have significant impact on the non-Darcy mixed convection under LTNE conditions.

**Keywords**—buoyancy ratio, mixed convection, non-Darcy model, thermal non-equilibrium

## I. INTRODUCTION

**T**HE study of double diffusive mixed convection in fluid saturated porous media has substantially increased during recent years because of its wide range of application, from the solidification of binary mixtures to the migration of solutes in water saturated soils. The other examples include geophysical system, hydrothermal vents and hot springs etc. A deep monograph to the various aspects of convection in porous medium is presented by Nield and Bejan [1] and Vafai [2]. The most of the former works on convective heat transfer in porous medium were under the assumption that the solid and fluid phases are in local thermal equilibrium (LTE) state. Generally, it is not true in some applications such as media in which the temperatures of solid and fluid phases are no longer identical [3]. In this situations the temperature of fluid and solid phases are accounted separately, therefore two energy equations emerge to represent each phase. This situation is known as local thermal non-equilibrium (LTNE) state.

Manish K. Khandelwal and P. Bera are with the Department of Mathematics, Indian Institute of Technology Roorkee, Roorkee, 247667, India.

A. Chakrabarti is with the Department of civil Engg., Indian Institute of Technology Roorkee, Roorkee, 247667, India.

\* Corresponding author: [mg\\_khandelwal@yahoo.co.in](mailto:mg_khandelwal@yahoo.co.in)

Recently, Khandelwal et al. [4] have studied the non-Darcy fully developed mixed convection in a vertical channel filled with porous media under the thermal non-equilibrium model. They have found that inter phase heat transfer coefficient ( $H$ ) smooths out the flow profile by removing point of inflection as well as flow separation on it, i.e. it stabilizes the basic state. However, effect of thermal conductivity ratio ( $\gamma$ ) is reverse. It is then natural to study how will the flow dynamics modulated on the consideration of solute transport in [4]. Based on this, in present study a fully developed double diffusive mixed convection along with LTNE assumption in a vertical porous channel is investigated by using non-Darcy-Brinkman-Forchheimer. A brief literature review on thermal convection has presented in [4], under the assumption of LTE and LTNE. Under the references of this, we have presented only recent articles on double-diffusive mixed convection in vertical geometry.

Bera et al. [5] have investigated stability properties on double-diffusive mixed convection in a vertical channel filled with a porous medium. They have found in two dimensional flow all compound within the hot vent fluid and the pore-water in the sediment undergo exchange, and the concept of unidirectional hot vent flows breaks down. An analytical and numerical study of mixed convection heat and mass transfer of a binary fluid in a vertical channel is examined by Alloui et al. [6]. They have discussed the possible existence of reverse flow in the channel. Double-diffusive mixed convection in a vertical pipe under local thermal non-equilibrium state has been investigated by Bera et al.[7]. They have found that, a kind of distortion appears on velocity profile, when buoyancy forces are opposing to each other. They have also shown that, for  $N < 0.7$ , there exists a minimum value of  $H$  such that the kind of distortion dies out i.e. velocity profile becomes free from flow separation.

## II. MATHEMATICAL MODEL

A fully developed double-diffusive mixed convective flow in a vertical channel filled with porous medium is considered. The flow caused by an external pressure gradient and two buoyancy forces (due to temperature and concentration differences). The wall temperature and concentration are assumed to vary linearly with  $x$  as  $T_w = T_0 + C_1x$  and  $C_w = C_0 + C_2x$ , where  $C_1$  and  $C_2$  are constant and  $T_0$  and  $C_0$  are the upstream reference temperature concentration respectively (see Fig. 1). The temperature of fluid and solid

phases are defined by different energy equation i.e a local thermal non-equilibrium model is adopted. Density is kept constant except in the buoyancy term in the momentum equation, which is satisfied by the Boussinesq approximation. The governing equations are written under assumption of non-Darcy-Brinkman-Forchheimer extended model [1].

Using the non-dimensional quantities  $x^* = x/L, y^* = y/L, z^* = z/L, P^* = PL^2/\rho_f \tilde{\nu}^2, t^* = t\tilde{\nu}P_g/L^2, V^* = VL/\tilde{\nu}P_g, \theta_f = (T_f - T_w)/C_1 LPr^* P_g, \theta_s = (T_s - T_w)/C_1 LPr^* P_g,$  and  $\Phi = (C - C_w)/C_2 LScP_g,$  the non-dimensional governing equations are given by

$$\nabla \cdot \mathbf{V}^* = 0 \tag{1}$$

$$\frac{P_g}{\varepsilon} \frac{\partial V^*}{\partial t^*} + \frac{P_g}{\varepsilon^2} (\mathbf{V}^* \cdot \nabla) \mathbf{V}^* = -\frac{1}{P_g} \nabla P^* - F|V^*|V^* + Ra_T^* (\theta_f + N\Phi) \vec{e}_x + \nabla^2 V^* - \frac{1}{Da^*} V^* \tag{2}$$

$$\frac{\partial \theta_f}{\partial t^*} + \frac{1}{\varepsilon} \left( u^* \frac{\partial \theta_f}{\partial x^*} + v^* \frac{\partial \theta_f}{\partial y^*} + w^* \frac{\partial \theta_f}{\partial z^*} \right) = \frac{1}{Pr^* P_g} \left( \frac{\partial^2 \theta_f}{\partial x^{*2}} + \frac{\partial^2 \theta_f}{\partial y^{*2}} + \frac{\partial^2 \theta_f}{\partial z^{*2}} - \frac{u^*}{\varepsilon} \right) + \frac{H(\theta_s - \theta_f)}{Pr^* P_g} \tag{3}$$

$$\Gamma \frac{\partial \theta_s}{\partial t^*} = \frac{1}{Pr^* P_g} \left( \frac{\partial^2 \theta_s}{\partial x^{*2}} + \frac{\partial^2 \theta_s}{\partial y^{*2}} + \frac{\partial^2 \theta_s}{\partial z^{*2}} \right) + \frac{\gamma H(\theta_f - \theta_s)}{Pr^* P_g} \tag{4}$$

$$\varepsilon \frac{\partial \Phi}{\partial t^*} + \left( u^* \frac{\partial \Phi}{\partial x^*} + v^* \frac{\partial \Phi}{\partial y^*} + w^* \frac{\partial \Phi}{\partial z^*} \right) = \frac{1}{ScP_g} \left( \frac{\partial^2 \Phi}{\partial x^{*2}} + \frac{\partial^2 \Phi}{\partial y^{*2}} + \frac{\partial^2 \Phi}{\partial z^{*2}} - u^* \right) \tag{5}$$

in which  $P_g = -\frac{dP^*}{dx}, Da^* = \frac{\tilde{\mu}K}{\mu_f L^2}, F = \frac{C_F L P_g}{K^{1/2}}, Ra_T^* = \frac{g\beta_T C_1 L^4}{\nu k_f}, Ra_S^* = \frac{g\beta_S C_2 L^4}{\nu D}, Pr^* = \frac{\tilde{\nu}}{\alpha_f}, Sc = \frac{\tilde{\nu}}{D}, N = \frac{Ra_S}{Ra_T}, H = \frac{hL^2}{\varepsilon k_f}, \gamma = \frac{\varepsilon k_f}{(1-\varepsilon)k_s}, \Gamma = \frac{\alpha_f}{\alpha_s}$  and  $\vec{e}_x$  are pressure gradient, modified Darcy number, Forchheimer number, modified thermal Rayleigh number, modified solutal Rayleigh number, modified Prandtl number, Schmit number, buoyancy ratio inter-phase heat transfer coefficient, porosity-scaled thermal conductivity ratio, diffusivity ratio and unit vector along vertical direction, respectively. The equation of motion are to be completed by the boundary conditions:  $V^* = 0, \theta_f = \theta_s = \Phi = 0$  at  $y = \pm 1$ .

Since the objective of the paper is to understand the flow dynamics as well as heat transfer mechanism of the steady, unidirectional fully developed flow, therefore, the above governing differential equations are reduced into the following set of coupled ordinary differential equations. (asterisks neglected).

$$1 - \frac{1}{Da} U_f - F|U_f|U_f + Ra_T(\Theta_f + N\Phi_0) + \frac{d^2 U_f}{dy^2} = 0 \tag{6}$$

$$\frac{d^2 \Theta_f}{dy^2} - \frac{U_f}{\varepsilon} + H(\Theta_s - \Theta_f) = 0 \tag{7}$$

$$\frac{d^2 \Theta_s}{dy^2} + \gamma H(\Theta_f - \Theta_s) = 0 \tag{8}$$

$$\frac{d^2 \Phi_0}{dy^2} = U_f \tag{9}$$

with boundary conditions  $U_f = \Theta_f = \Theta_s = \Phi_0$  at  $y = \pm 1$ , where  $U_f, \Theta_f, \Theta_s,$  and  $\Phi_0$  are the base velocity, base fluid temperature, base solid temperature and base concentration respectively. Above basic state equations (6)-(9) along with boundary condition are solved numerically by using the spectral Chebyshev collocation method. The details of this method and implementation can be found in ([8], [4]).

The rates of heat as well as mass transfer are determined in

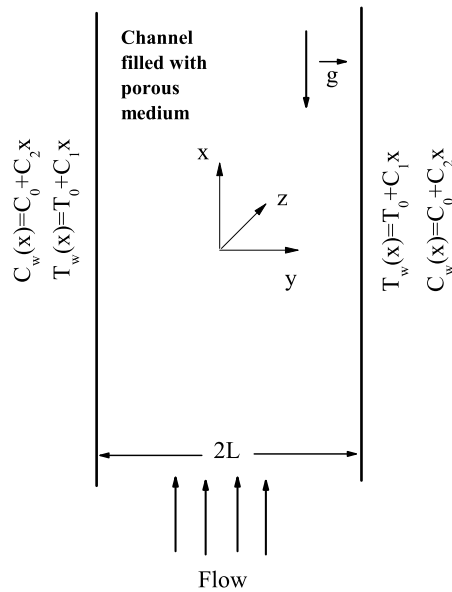


Fig. 1. Schematic diagram of the physical problem and coordinate system.

terms of bulk temperature and concentration. The local Nusselt numbers for fluid ( $Nu_f$ ), as well as solid ( $Nu_s$ ) and Sherwood ( $Sh$ ) are defined as:

$$Nu_f = 2L \frac{\frac{\partial T_f}{\partial y}|_{y=L}}{\left( T_w - \frac{\int_{-L}^L U_f T_f dy}{\int_{-L}^L U_f dy} \right)} \tag{10}$$

$$Nu_s = 2L \frac{\frac{\partial T_s}{\partial y}|_{y=L}}{\left( T_w - \frac{\int_{-L}^L U_f T_s dy}{\int_{-L}^L U_f dy} \right)} \tag{11}$$

$$Sh = 2L \frac{\frac{\partial \Phi}{\partial y}|_{y=L}}{\left( T_w - \frac{\int_{-L}^L U_f \Phi dy}{\int_{-L}^L U_f dy} \right)} \tag{12}$$

These integrals are evaluated by Gauss-Chebyshev quadratures formula.

## III. RESULTS AND DISCUSSION

In this section, the heat and solute transfer and fluid flow are governed by thermal Rayleigh number ( $Ra_T$ ), Darcy number ( $Da$ ), Forchheimer number ( $F$ ), buoyancy ratio ( $N$ ), inter phase heat transfer coefficient ( $H$ ), porosity scaled thermal conductivity ratio ( $\gamma$ ) and porosity ( $\epsilon$ ). Here, our objective is to investigate the effect of buoyancy ratio ( $N$ ) and thermal non-equilibrium parameter ( $H$ ) on the heat and mass transfer and fluid flow profiles. Based on this, we have fixed other parameters  $Da$ ,  $F$ ,  $\gamma$ , and  $\epsilon$ , at  $10^{-3}$ , 100, 0.01 and 0.97 respectively. An important note must be made regarding to buoyancy ratio ( $N$ ) in the present study. Here in the entire study buoyancy ratio has been considered as a positive value. From our base equation, the positive (Negative) value of  $Ra_T$  shows that two buoyancy forces are in favor (against) of each other i.e. the thermal and solutal forces make aiding (opposing) contribution of each other. Therefore, two value of  $Ra_T$  is fixed at 1000 and -1000. The range of  $H$  and  $N$  is considered  $[10^{-1}, 10^3]$  and  $[0, 100]$  respectively. Before discussing the impact of different above parameters on mixed convection, a code validation is given. The numerical code is a modification of the code generated by Khandelwal et al. [4] for the present problem. We have compared our results with published results of Chen et al. [9]. He has obtained the Nusselt number for  $Ra_T = 1000$  and  $Da = 10^{-2}$  and  $F = 0$ , in single diffusive case. Its corresponding value is 8.45. The same is also calculated for  $N = 0$ ,  $H = 0$  and given by 8.44. It can be seen from the comparison with the present work is in a good agreement with previous work.

In case of aiding (two buoyancy forces are in favor,  $Ra_T = 1000$ ) the variation of the Nusselt number (fluid ( $Nu_f$ ) and solid ( $Nu_s$ )) as well as Sherwood number ( $Sh$ ) as function of  $H$  for different values 0, 1, 10 and 100 of  $N$  are plotted in Fig.2 (a)-(c). Following observations can be pointed out from the above figure. First, for a given value of  $N$  the heat transfer rate of fluid ( $Nu_f$ ) increases significantly in a small interval of  $H$  (starting from zero), and it attains maximum value at a certain value of  $H$ , and denoted by  $H_0$ . Beyond  $H_0$ , the  $Nu_f$  decreases smoothly and converge to a constant value (See Fig.2(a)). Second, increasing of buoyancy ratio results increasing of  $Nu_f$ . Third, the solid heat transfer rate  $Nu_s$  shows constant behavior in  $[0, H_0]$  for  $N = 0$  and 1, beyond that it increases. However, for  $N = 10$  and 100  $Nu_s$  increases significantly and converge to a constant (See Fig.2(b)). Forth, the variation of the Sherwood number ( $Sh$ ) decreases on increasing  $H$  and converge to constant for a given value of  $N$ . The  $Sh$  in ( $H$ ,  $Sh$ )-plane is almost constant for  $H > 50$ .

A qualitative explanation for the physics involved behind above phenomena can be explained by the definition of  $H$  and  $\gamma$ . On fixing the other parameters, increasing of  $H$ , increases the volumetric inter phase heat transfer coefficient. Therefore, in the beginning it is expected that heat transfer of fluid as well as solid will be enhanced on increasing  $H$ . As  $H$  is increased beyond a threshold value ( $H_0$ ), the heat transfer in between fluid to solid will be reduced. At the same time, the heat transfer characteristic in solid is expected to be reverse beyond

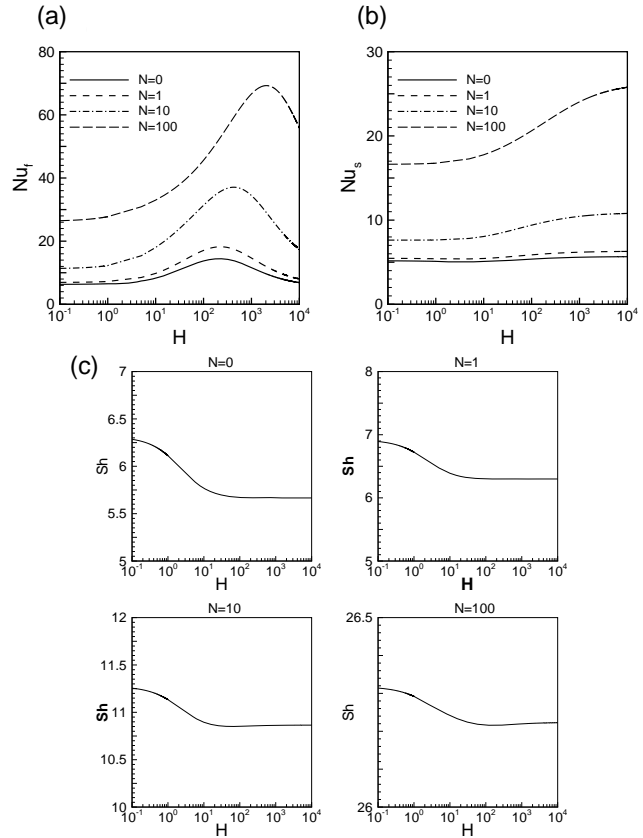


Fig. 2. Representation of  $Nu/Sh$  as a function of  $H$  for different value of  $N$  at  $Ra_T = 1000$ ,  $Da = 10^{-3}$ ,  $F = 100$  and  $\gamma = 0.01$ .

the threshold value of  $H$ . For higher values of  $H$  both fluid as well as solid will approach to equilibrium state i.e. both media will not exchange the heat. Therefore a smooth decay/increase of  $Nu_f/Nu_s$  is also expected beyond  $H_0$ .  $\gamma = 0.01$  and porosity 0.97 imply conductivity of solid is 3300 times conductivity of fluid, which implies that diffusivity of solute is less compare to diffusivity of fluid. Consequently of it, for  $N = 10, 100$  solid heat transfer rate increases on increasing  $H$ , and mass transfer rate due to LTNE does not much more effective for given  $N$ .

Similarly, for opposing flow ( $Ra_T = -1000$ ), the variation of the Nusselt number ( $Nu_f$  and  $Nu_s$ ) as well as Sherwood number ( $Sh$ ) as a function of  $H$  for different values 0, 1, 10 and 100 of  $N$  is plotted in Fig. 3(a)-(c). As can be observed from the above figures, for  $N = 0, 1$  the  $Nu_f$  is same as  $Ra_T = 1000$ , whereas it is reverse for  $N = 10$  and 100. The solid heat transfer rate and for  $N = 0, 1$  and 10 increases on increasing  $H$  and converge to a constant value. However for  $N = 100$  it is reverse and converge to constant value. The variation of  $Sh$  in ( $H$ ,  $Sh$ )-plane is similar to variation of  $Nu_s$  in ( $H$ ,  $Nu_s$ )-plane, for  $N = 0$  and 1, but for  $N = 100$  it is reverse. In case of  $N = 10$ , the magnitude of  $Sh$  decreases on increasing  $H$  from 0 to  $H_0$ , and beyond it the same starts to increase as a function of  $H$ . It is also pointed that the magnitude of  $Sh$  does not much more effective on increasing  $H$  (see Fig.3(b) and 3(c)).

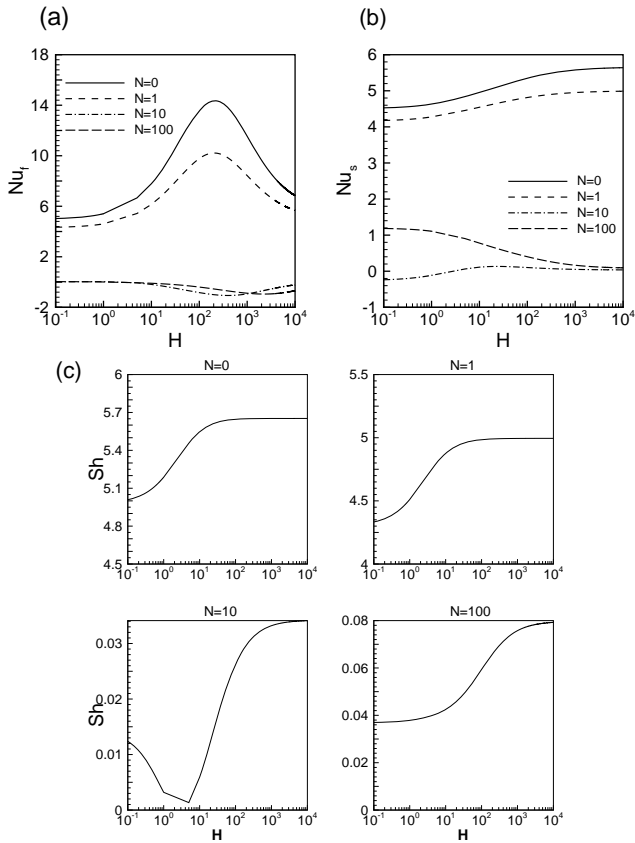


Fig. 3. Representation of  $Nu/She$  as a function of  $H$  for different value of  $N$  at  $Ra_T = -1000$ ,  $Da = 10^{-3}$ ,  $F = 100$  and  $\gamma = 0.01$ .

To understand the the physics behind this anomaly, variation of velocity as a function of  $N$  is plotted in Fig. 4. For  $N = 0$  and  $1$ , the velocity profile is free from point of inflection. However, for  $N = 10$  and  $100$  the profile contains the point of inflection i.e the profiles possess back flow tendency. In case of  $N = 100$ , variation of velocity profile shows a sinusoidal pattern and the number of zeroes increase. Similarly the temperature as well as concentration profile contains point of inflection (Fig. is not shown).

As can be seen that from the above figure, the velocity profile possesses a kind of distortion [4], [8]. The existence of the flow separation as well as inflection point on velocity profile shows the instability of the flow [10], [11]. Therefore, in this situation, assuming flow (fully developed and unidirectional) is not realistic. Hence, above unfavorable results (in Nusselt and Shearwood number) may be the consequence of it. Furthermore, the back flow and number of zeroes increase on increasing  $N$ . As a result, it can be concluded that  $N$  destabilize the flow.

To more explanation in this direction, a study of the variation of heat transfer rate at the wall,  $Nu_f$ , in  $(N, Nu_f)$ -plane is required. It has been observed that in case of aiding flow ( $Ra_T = 1000$ ),  $Nu_f$  varies smoothly as an increasing function of  $N$  (see Fig. 5(a)), whereas, in case of opposing flow ( $Ra_T = -1000$ ) the variation of  $Nu_f$  is similar to a sinusoidal form

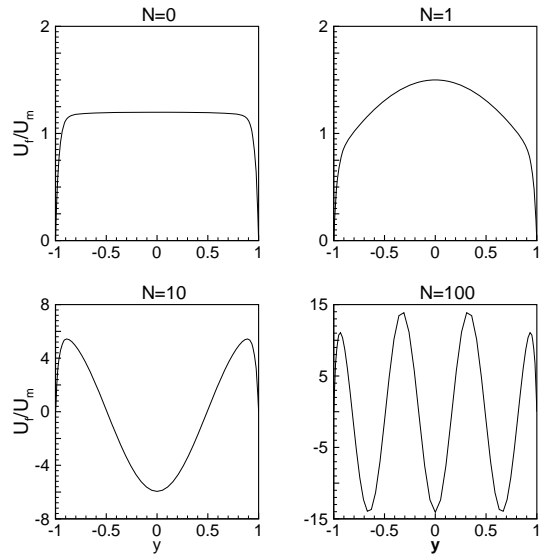


Fig. 4. Velocity profiles of flow for different value of  $N$  at  $Ra_T = -1000$ ,  $Da = 10^{-3}$ ,  $F = 100$ ,  $\gamma = 0.01$ , and  $H = 30$ .

(see Fig. 5(b)). Similarly type observation is also obtained for  $Nu_s$  and  $Sh$  (figure is not shown) . Therefore, the domain of  $N$  can be divided into finite number of sub domain, such that, in each sub domain  $Nu_f$  attains a maximum and a minimum value. The length of the sub interval increases on increasing  $N$ .

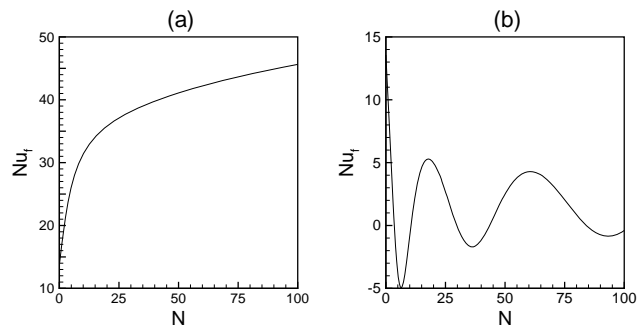


Fig. 5. Variation of the Nusselt number ( $Nu_f$ ) as a function of  $N$  at  $Da = 10^{-3}$  and  $F = 100$ ,  $H = 100$  and  $\gamma = 0.01$ : (a)  $Ra_T = 1000$  and (b)  $Ra_T = -1000$  .

Apart from this, for  $N \leq 0.1$ , there exist a minimum value of  $H$  such that velocity profile becomes free from point of inflection, when  $Ra_T = 1000$ . However, for  $N \geq 0.1$  the velocity profile always contains point of inflection for any value of  $H$ . This shows that solutal buoyancy force is dominated over thermal buoyancy force, i.e.  $N$  destabilizes the flow.(see Fig.6 (a))

Similarly, for opposing flow ( $Ra_T = -1000$ ), it is found that, the flow separation as well as point of inflection does not appear for  $N \leq 1.6$  and  $H = 0$ , or the flow separation as well as point of inflection appears for  $N > 1.6$  and  $H = 0$ . In this situation, for  $N \leq 2.8$ , there exist a minimum value of  $H$  such that the velocity profile becomes free from inflection

point as well as flow separation. But for  $N \geq 2.9$ , the velocity profile contains flow separation for any value of  $H$ . At  $N = 7.2$  velocity profile is changed as upside down (see Fig.6 (b)). This type of sudden change shows that, in this situation assuming flow is fully developed and unidirectional is not realistic.

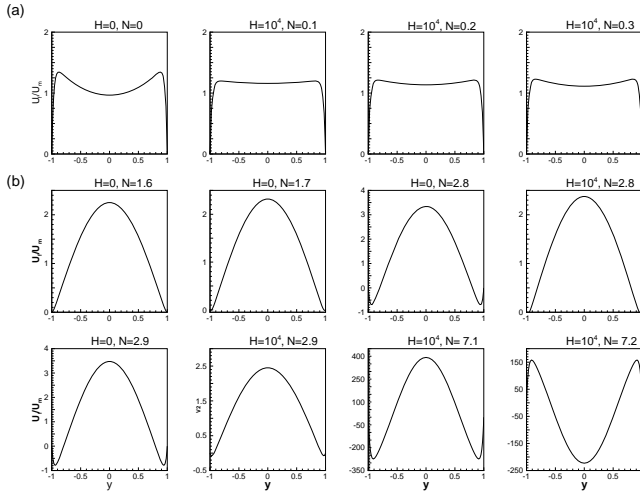


Fig. 6. Velocity profiles of flow for different value of  $N$  and  $H$  at  $Da = 10^{-3}$ ,  $F = 100$  and  $\gamma = 0.01$ : (a)  $Ra_T = 1000$  and (b)  $Ra_T = -1000$ .

#### IV. CONCLUSIONS

We have studied a fully developed double diffusive mixed convective flow in a vertical porous channel by using the local thermal non-equilibrium (LTNE) model. The non-Darcy-Brinkman-Forchheimer extended model has been used. The governing equations are solved by numerically by Spectral collocation method. The main emphasize is given on combine influence of two buoyancy forces in terms of  $N$  as well as LTNE parameter  $H$  on appearance of point of inflection/flow separation on the flow profile. The following remarks can be made from detailed results.

- When both the buoyancy forces thermal as well as solutal are in favor of each other ( $Ra_T = 1000$ ), the heat transfer rate of fluid ( $Nu_f$ ) increases upto a certain value of  $H$ , beyond that decreases smoothly and converge to a constant value. However, in case of opposing flow ( $Ra_T = -1000$ ), the result is same as above for  $N = 0$  and  $1$ , and reverse for  $N = 10$  and  $100$ .
- In case of aiding flow the variation of Sherwood number( $Sh$ ) decreases on increasing  $H$  and converge to constant for all given value of  $N$ , whereas for opposing flow it is reverse for  $N = 0, 1$  and  $100$ .
- Variation of  $Nu_f$  in the  $(N, Nu_f)$ -plane shows a sinusoidal form for opposing flow ( $Ra_T = -1000$ ), whereas for aiding flow, the same shows as a smooth increasing function.
- The velocity profile contains point of inflection as well as flow separation on increasing  $N$  i.e  $N$  destabilizes the flow.
- Overall, the buoyancy force have significant effect on the non-Darcy mixed convection under LTNE conditions.

#### ACKNOWLEDGMENT

One of the authors, Manish K. Khandelwal, is grateful to Council of Scientific and Industrial Research (CSIR) India for providing financial support during the preparation of this manuscript. Author Manish K. Khandelwal acknowledges Department of Science and Technology (DST) India for providing financial support to present this work in International Conference on Computational Fluid Dynamics, Paris France.

#### REFERENCES

- [1] D.A. Nield and A. Bejan, *Convection in Porous Media*, Springer, New York, 2006.
- [2] K. Vafai, *Handbook of Porous Media*, Marcel Dekker, New York, 2000.
- [3] V.V. Calmidi and R.L. Mahajan, "Forced convection in high porosity foams", *Trans. ASME J. of Heat Transfer*, vol. 122 pp. 557-565, 2000.
- [4] M.K. Khandelwal and P. Bera, "A thermal non-equilibrium perspective on mixed convection in a vertical channel", *Int. J. Thermal Sciences* vol. 56 pp. 23-34, 2012.
- [5] P. Bera, J. Kumar and A. Khalili, "Hot springs mediate spatial exchange of heat and mass in the enclosed sediment domain: A stability perspective", *Adv. Water Resources*, vol. 34 pp. 817-828, 2011.
- [6] Z. Alloui and P. Vasseur, "Fully developed mixed convection of a binary fluid in a vertical porous channel", *The canadian J. Chem. Engineering*, 1-9, 2012.
- [7] P. Bera, S. Kapoor and M.K. Khandelwal, "Double-diffusive mixed convection in a vertical pipe: a thermal non-equilibrium approach" accepted for publication in *Int. J. Heat and Mass Transfer* (2012).
- [8] A. Kumar and P. Bera J.Kumar "Non Darcy mixed convection in a vertical pipe filled with porous medium", *Int. J. of Thermal Sciences* vol. 50 pp. 725-735, 2011.
- [9] Y.C. Chen, J.N. Chung, C.S. Wu and Y.F. Lue, "Non-Darcy flow stability of mixed convection in a vertical channel filled with a porous medium" *Int. J. Heat Mass Transfer* vol. 43 pp. 2421-2429, 2000.
- [10] P.G. Drazin and W.H. Reid, *Hydrodynamic Stability* Cambridge: Cambridge University Press; 2004.
- [11] Y.C. Su and J.N. Chung, "Linear stability analysis of mixed-convection flow in a vertical pipe", *J. Fluid Mechanics* vol. 422 pp. 141-166, 2000.